Published in final edited form as:
Curr Biol. 2014 April 14; 24(8): 822–831. doi:10.1016/j.cub.2014.03.021.

Dopaminergic modulation of cAMP drives nonlinear plasticity across the *Drosophila* mushroom body lobes

Tamara Boto[1], **Thierry Louis**[1], **Kantiya Jindachomthong**[2], **Kees Jalink**[3], and **Seth M. Tomchik**[1,†]

[1]Department of Neuroscience; The Scripps Research Institute, Scripps Florida; Jupiter, FL; USA [2]SURF Program; The Scripps Research Institute, Scripps Florida; Jupiter, FL; USA [3]Division of Cell Biology; The Netherlands Cancer Institute; Amsterdam; The Netherlands

SUMMARY

Background—Activity of dopaminergic neurons is necessary and sufficient to evoke learning-related plasticity in neuronal networks that modulate learning. During olfactory classical conditioning, large subsets of dopaminergic neurons are activated, releasing dopamine across broad sets of postsynaptic neurons. It is unclear how such diffuse dopamine release generates the highly localized patterns of plasticity required for memory formation.

Results—Here we have mapped spatial patterns of dopaminergic modulation of intracellular signaling and plasticity in *Drosophila* mushroom body (MB) neurons, combining presynaptic thermogenetic stimulation of dopaminergic neurons with postsynaptic functional imaging *in vivo*. Stimulation of dopaminergic neurons generated increases in cAMP across multiple spatial regions in the MB. However, odor presentation paired with stimulation of dopaminergic neurons evoked plasticity in Ca^{2+} responses in discrete spatial patterns. These patterns of plasticity correlated with behavioral requirements for each set of MB neurons in aversive and appetitive conditioning. Finally, broad elevation of cAMP differentially facilitated responses in the gamma lobe, suggesting that it is more sensitive to elevations of cAMP, and that it is recruited first into dopamine-dependent memory traces.

Conclusions—These data suggest that the spatial pattern of learning-related plasticity is dependent on the postsynaptic neurons' sensitivity to cAMP signaling. This may represent a mechanism through which single-cycle conditioning allocates short-term memory to a specific subset of eligible neurons (gamma neurons).

†Corresponding Author: Seth M. Tomchik, Department of Neuroscience, The Scripps Research Institute, Scripps Florida, 130 Scripps Way #3C1, Jupiter, FL 33458, Tel: (561) 228-3496, Fax: (561) 228-2250, stomchik@scripps.edu.

INTRODUCTION

Dopaminergic neurons are involved in modulating diverse behaviors, including learning [1–5], motor control [6], motivation [1, 7], arousal [8, 9], addiction and obesity [10], and salience-based decision-making [11, 12]. In *Drosophila*, dopaminergic neurons innervate multiple brain regions, including the mushroom body (MB), where they modulate aversive learning [3–5, 13–19], forgetting [20, 21], state-dependent modulation of appetitive memory retrieval [22], expression of ethanol-induced reward memory [23], and temperature preference behavior [24, 25].

Dopaminergic circuits play a particularly critical role in memory acquisition. During olfactory classical conditioning, where an odor (conditioned stimulus [CS]) is paired with an aversive event (e.g., electric shock; the unconditioned stimulus [US]), dopaminergic neurons respond strongly to the aversive US [15]. Dopamine functions in concert with activity-dependent Ca^{2+} influx to synergistically elevate cAMP [26] and PKA [27], suggesting that dopamine is one component of a molecular coincidence detector underlying learning. Proper dopamine signaling is necessary for aversive and appetitive memory [18, 28]. Moreover, driving activity of a subset of TH-GAL4+ dopaminergic neurons that differentially innervates the vertical α/α′ MB lobes (with less dense innervation of the horizontal β/β′/γ lobes, peduncle, and calyx), is sufficient to induce behavioral aversion to a paired odorant in larvae and adult flies [13, 16, 17, 29]. Conversely, stimulation of a different set of Ddc-GAL4+ dopaminergic neurons, the PAM cluster that innervates mainly the horizontal β/β′/γ lobes, is sufficient to induce behavioral attraction to a paired odorant [30, 31]. Thus, dopaminergic neurons comprise multiple circuits with distinct roles in memory acquisition.

Multiple subsets of MB neurons receive CS and US information and express molecules associated with the coincidence detection [4, 5], making them theoretically eligible to generate dopamine/cAMP-dependent plasticity. Yet only some subsets are required to support memory at any given time following conditioning [3, 19, 32–38], leaving open the question of how spatial patterns of plasticity are generated during conditioning. Here we have approached this question, using a novel technique to probe the postsynaptic effects of neuronal pathway activation. We paired odor presentation with stimulation of presynaptic dopaminergic neurons via ectopic expression of the heat-sensitive channel TRPA1, while monitoring postsynaptic effects with genetically-encoded optical reporters for Ca^{2+}, cAMP, and PKA *in vivo*.

RESULTS

Dopamine elevates cAMP and PKA across multiple spatial regions of the mushroom bodies

First we considered whether dopamine exerts uniform or differential effects across different spatial regions and subsets of mushroom body (MB) neurons. We used the GAL4-UAS system to express a genetically-encoded cAMP reporter, epac1-camps, in the adult MB. Two GAL4 lines were used to drive reporter expression: 238Y and c739. 238Y drives expression in all three class of MB neurons – α/β, α′/β′, and γ, with the most robust expression in α/β and γ neurons, while c739 drives robust expression only in MB α/β neurons (Figure 1A,B).

Multiple regions of the MB were imaged in isolated, intact brains with confocal microscopy. Distinct regions of interest were quantified, corresponding to the terminal regions of different subsets of afferent dopaminergic neurons [14, 15, 17, 29, 30].

When dopamine was applied in the bath, concentration-dependent increases in the inverse FRET ratio were observed across multiple regions of the MB, indicating a rise in cytosolic cAMP (Figure 1 C–G). Notably, these responses were observed in both the vertical lobes (α lobe tip, upper stalk and lower stalk) and horizontal lobes (heel, β, and γ lobes). To test whether the responses were due to activation of D1-like dopamine receptors, we imaged the responses in the α tip and β lobe to dopamine, in the presence of increasing concentrations of the competitive dopamine receptor antagonist SCH-23390 (Figure 1 E,H). This antagonist reversibly inhibited the cAMP responses evoked by dopamine in both regions. A previous study noted no change in PKA in the horizontal lobes when dopamine was applied [27]. To examine whether the cAMP elevation we observed translates into PKA responses, we examined dopamine-evoked responses of a PKA reporter, AKAR3. We observed concentration-dependent increases in PKA activity upon application of dopamine in the bath (Figure 1 I,J). Examination of the logEC50 values revealed a heightened sensitivity to dopamine at the α tip relative to other spatial regions of the MB in terms of both cAMP and PKA responses (Figure 1K). This suggests that either the α tip is intrinsically more sensitive to dopamine or that there is better access of dopamine to this superficial brain region, although all regions responded robustly. Overall, these data suggest that dopamine evokes increases in cAMP and PKA across multiple regions in both the vertical and horizontal MB lobes.

Multiple subsets of dopaminergic neurons elevate cAMP in discrete spatial patterns

Dopaminergic neurons innervate multiple spatial regions of the MB and modulate multiple learned and motivated behaviors, ranging from temperature preference to aversive and appetitive olfactory learning (Figure S1) [14, 17, 18, 22, 24, 25, 29–31]. This diversity in behavioral functions led us to question whether distinct sets of dopaminergic neurons exert different effects on postsynaptic cAMP levels across different postsynaptic terminal zones (e.g., via bidirectionally regulation of cAMP through actions on distinct pools of postsynaptic D1- and D2-like receptors). The MB calyx shows regionally-specific bidirectional effects of dopamine on cAMP [26], suggesting that spatial regulation may be important. To determine whether this occurs in the axonal lobes, which receive tiled innervation by dopaminergic neurons [14, 15, 17, 29, 39], we mapped the effects of stimulating different anatomical classes of dopaminergic neurons on postsynaptic cAMP concentrations across spatial compartments of the MB lobe *in vivo*. The genetically-encoded, FRET-based cAMP reporter $^{T}epac^{VV}$ was expressed in the MB using a 247-bp MB enhancer, henceforth termed MB-$^{T}epac^{VV}$. This imaging construct was used in combination with thermogenetic activation of different subpopulations of afferent dopaminergic neurons, driving the temperature-sensitive cation channel TRPA1 under UAS control with various GAL4 drivers (see Supplemental Experimental Procedures).

In this preparation, the bath temperature was ramped from 22°C to 32°C and back to transiently stimulate the dopaminergic neurons while imaging the postsynaptic cAMP

concentrations with MB-^{T}epac^{VV} (Figure 2C). We first stimulated a group of dopaminergic neurons driving TRPA1 with the tyrosine hydroxylase GAL4 (TH-GAL4). This driver labels the PPL1 cluster, which innervates a large swath of the vertical lobes and junction, as well as a subset of PAM neurons innervating the horizontal/medial lobes, PPL2ab neurons that innervate the calyx, and some other regions of the protocerebrum and central complex [14, 15, 17, 29, 39, 40]. Six z planes were imaged, allowing us to visualize the responses across all MB spatial zones that are innervated by these dopaminergic neurons (Figure 2 A,B). Increases in the inverse FRET ratio were observed during the transient heating in flies expressing the reporter in the MB (TH-GAL4>UAS-TRPA1), corresponding to an elevation of cAMP (Figure 2 D–F). There were significant differences between the response magnitudes across both regions and genotypes ($p < 0.001$, two-way ANOVA), and the control groups were not significantly different from one another ($p > 0.05$; Tukey tests). Responses in the TH-GAL4>UAS-TRPA1 flies were significantly larger than controls lacking one or both components of the bipartite expression system across all regions of the vertical lobes (Figure 2F), but did not reach significance relative to some controls in the γ lobe or heel. This pattern corresponds well with the anatomical innervation of the MB by the neurons in the TH driver (heavier in the vertical lobes) (Figure S1) [14, 15].

To further refine the stimulation pattern, we drove TRPA expression in smaller subsets of dopaminergic neurons with additional GAL4 drivers, comparing the responses to the respective GAL4/+ controls (Figures 3A, S1). The C150 driver labels the V1, MV1, and MP1 neurons innervating the MB upper stalk, lower stalk, and heel [41]. Upon stimulation of this subset of neurons, we observed increases in cAMP in the upper and lower stalk (with a trend in the heel), but not the α, α′ or β/γ regions (Figure 3B). The NP7198 driver labels V1 neurons innervating the upper stalk [14]. Stimulating these neurons with TRPA resulted in significant increases in cAMP in the upper stalk, but nowhere else in the MB (Figure 3C). The V1/MV1 driver NP2755 was also tested, revealing significant increases in cAMP in the lower stalk, upper stalk, and β lobe (Figure 3D). The MP1 driver C061 produced a significant increase in cAMP in the heel, but nowhere else (Figure 3E). Finally, we tested the Ddc-GAL4 driver, which labels the PAM cluster of dopaminergic neurons that innervate the horizontal lobes of the MB [39, 42], and are necessary and sufficient to drive appetitive learning [30, 31]. Stimulation of these neurons revealed a large increase in cAMP in the horizontal β and γ lobes and the lower stalk, but not the other regions (Figure 3F). These data collectively demonstrate that multiple different subsets of dopaminergic neurons elevate cAMP in a compartmentalized fashion within the MB neurons, in spatial patterns that precisely mimic the innervation pattern of the dopaminergic neurons. All drivers tested produced increases in cAMP; we could discern no qualitative differences in the effects of different subsets of dopaminergic neurons in terms of postsynaptic actions on cAMP.

Stimulation of dopaminergic neurons reveals a spatial dissociation between cAMP and plasticity

The broad elevation of cAMP we observed raised the question of how localized the dopamine-evoked plasticity could be within the MB. As elevating cAMP acutely enhances MB neuron excitability [26], broad elevation of cAMP might be expected to enhance excitability broadly across the MB. In addition, many dopaminergic neurons are expected to

be simultaneously active during classical conditioning, as they exhibit overlapping, phasic patterns of activity in response to sensory stimuli [15, 25]. To examine the dopamine-induced plasticity in the MB, we paired odor presentation with stimulation of dopaminergic neurons, imaging Ca^{2+} responses to odor pre- and post-pairing with GCaMP3. Changes in these responses are henceforth termed Ca^{2+} response plasticity. Flies were generated that contained a GAL4 driver, UAS-TRPA1, and MB-GCaMP3 (constitutively expressing GCaMP3 in the MB). For each experiment, a fly was immobilized in an imaging chamber and an odor was presented across three trials while imaging Ca^{2+} activity in the MB *in vivo* (Figures 4, S2, S3). After the second odor presentation, a conditioning paradigm was carried out, in which the odor was presented for 30 s while the bath temperature was ramped to 32°C to activate dopaminergic neurons (Figure 4D). Following conditioning, odor responses were imaged again, and the responses before and after conditioning were compared (Figure 4E–I). This paradigm was designed to mimic olfactory classical conditioning, in which pairing odor with stimulation of TH-GAL4-positive dopaminergic neurons (henceforth TH-GAL+) produces aversive behavioral memory or, conversely, pairing odor with Ddc-GAL4+ neuron stimulation produces appetitive memory [16, 17, 29–31].

In the first set of experiments, we stimulated TH-GAL4+ dopaminergic neurons. Although there is strong dopaminergic innervation of the MB vertical lobes with this driver and strong elevation of cAMP in this region following TH-GAL4>TRPA stimulation (Figure 2), we found no significant change in the odor-evoked Ca^{2+} responses in the α tip, α′ tip, upper stalk, lower stalk, β lobe, or heel following conditioning (Figure 4 F,H,I, S2, S3). However, in contrast, we observed a striking increase in odor-evoked Ca^{2+} responses in the γ lobe following conditioning (Figure 4 E,G–I, S2, S3, Movie S1). This was not observed with backward conditioning, where the odorant was presented following stimulation of dopaminergic neurons (Figure 4 D,H,I, S3). In addition, there was no effect in control experiments, where heat was omitted or flies lacked either the GAL4 or UAS element (Figure 4 H,I, S3). Therefore, we conclude that the Ca^{2+} response plasticity in the γ lobe was specifically due to coincident reception of odor and stimulation of dopaminergic neurons via TRPA. These data demonstrate that while the largest increases in cAMP occurred in the vertical lobes following stimulation of the TH-GAL4+ dopaminergic neurons, the Ca^{2+} response plasticity evoked by conditioning was confined to the γ lobe.

The localization of this dopamine-dependent plasticity to the γ lobe raised the question of where appetitive dopamine-dependent plasticity is localized, considering that the appetitive memory-related PAM neurons innervate the horizontal β/γ lobes. Consequently, we tested the effect of stimulating the PAM cluster of dopaminergic neurons in a similar conditioning paradigm. Upon stimulation of PAM neurons by driving TRPA1 with the Ddc-GAL4 driver, we again observed a significant increase in Ca^{2+} responses in the γ lobe between the forward conditioned and all other groups (Figure 5, S2, S3). However, in contrast to the precise localization observed with the TH driver, a change was observed across multiple MB regions: the γ lobe, α tip, α′ tip, upper stalk, lower stalk, and heel (Figure 5 B–D, S2, S3). This difference was reflected in both significant increases in the magnitudes of odor responses in all regions (except the β lobe) following forward conditioning, as well as significant decreases in responses in the α tip, upper stalk, lower stalk, and heel regions

following backward pairing. Thus, although stimulation of PAM neurons with the Ddc-GAL4 driver produces detectable elevations of cAMP only in the horizontal β and γ lobes, the Ca^{2+} response plasticity was observed across a wider group of MB neurons.

The Ddc-GAL4 driver exhibits expression in both dopaminergic and serotonergic neurons [42, 43], although the neurons innervating the MB in this driver are largely dopaminergic [30]. To further test whether the Ca^{2+} response plasticity was due specifically to dopaminergic neuron stimulation, we utilized an additional PAM neuron driver, R58E02, which expresses GAL4 in only dopaminergic PAM neurons [30]. When pairing odor presentation with stimulation of PAM neurons with this driver, we again observed a significant increase in odor responses in the γ lobe (Figure 5D). Also, in concurrence with results from the Ddc driver, stimulation with R58E02 revealed both an increase in odor-evoked Ca^{2+} responses following forward conditioning and a decrease following backward conditioning in the α tip (Figure 5D, S2). These data provide further confirmation that stimulation of dopaminergic PAM neurons during odor presentation produces Ca^{2+} response plasticity in the MB.

The MB γ lobe is differentially sensitive to cAMP

The spatial dissociation of cAMP elevation and plasticity in the MB, particularly the strikingly restricted pattern of facilitation following stimulation of TH-GAL4+ dopaminergic neurons, raised the question of how such specificity may be generated. We hypothesized that the sensitivity of the postsynaptic neurons (the MB neurons) to elevations of cAMP may determine their pattern of recruitment into the dopamine-dependent plasticity, and that the γ lobe neurons are intrinsically more sensitive to elevation of cAMP than neurons in the other lobes. To test this, we imaged odor responses in the MB before and after applying forskolin in the bath solution to elevate cAMP levels broadly in the brain. The 238Y-GAL4 driver was used to express UAS-GCaMP6f in the MB for imaging. To mimic our previous conditioning paradigm, odor responses were imaged twice, followed by a conditioning period with 30s of odor paired with 30s of forskolin (or the control drug 1,9-dideoxyforskolin, which does not elevate cAMP and also serves as a vehicle control here), and then another odor presentation (Figure 6, S3). The lowest concentration of forskolin (1 μM) produced no change in post-pairing odor responses in any region of the MB imaged (Figure 6 A,B), and likewise there was no change in odor responses if it was omitted (i.e., a 30-s unpaired odor presentation had no effect) (Figure 6, S4). Application of forskolin at higher concentrations (10, 30, and 100 μM) produced significant increases in the post-forskolin odor responses in the γ lobe, as well as the heel at 100 μM (Figure 6 A,B, S3). The post/pre odor response ratios differed significantly between the forskolin and 1,9-dideoxyforskolin control groups in the γ lobe and heel at 30 μM and 100 μM (Figure 6B, S3).

To further test whether forskolin-induced facilitation was excluded from the α/β and α′/β′ neurons, we expressed GCaMP6f in each of these MB subdivisions with specific drivers. The GAL4 driver c739 was used to image Ca^{2+} responses in α/β neurons, and c305a was used to image α′/β′ neurons. No significant change in responses was observed in the α tip or β lobe following pairing of odorant with forskolin at 30 μM or 100 μM (Figure 6C).

Similarly, no significant changes in odor response magnitudes were observed in the α′ tip or β′ lobe following pairing of odorant with either concentration of forskolin (Figure 6C). To rule out the possibility that these results were due to more effective forskolin-induced elevation of cAMP in the γ lobe, we compared forskolin-induced elevations of cAMP in the α tip and γ lobe in 238Y-GAL4>UAS-epac1-camps flies. Forskolin effectively elevated cAMP in both regions, and in fact increased cAMP slightly more in the α tip (Figure 6D). Therefore, using three GAL4 drivers, we observed cAMP-induced short-term Ca^{2+} response plasticity only in the γ lobe, suggesting that it is differentially facilitated by cAMP elevation.

Finally, we tested whether odor reception was necessary for cAMP-induced facilitation by omitting the odor presentation during application of forskolin and imaging the γ lobe in 238Y>GCaMP6f flies (Figure S4). Odor-evoked Ca^{2+} responses in the γ lobe were facilitated in the absence of odor presentation, suggesting that direct activation of adenylyl cyclases at least partially bypasses the coincidence detection machinery in the MB [5]. Overall, these data suggest that the γ lobe is particularly sensitive to elevations of cAMP produced during single-cycle conditioning, and therefore differentially exhibits short-term dopamine-dependent plasticity. Thus, the cAMP sensitivity of the postsynaptic (MB) neurons may be a critical factor in determining which neurons are recruited into a memory trace during salient sensory events.

DISCUSSION

The present data demonstrate four major points about how dopaminergic circuits function in neuronal plasticity underlying olfactory classical conditioning. (I) Stimulation of small subsets of dopaminergic neurons evokes consistent, compartmentalized elevations of cAMP across the MB lobes. (II) Broad stimulation of dopaminergic neurons generates broad postsynaptic elevation of cAMP, but Ca^{2+} response plasticity occurs in discrete spatial regions. (III) Stimulation of TH-GAL4+ neurons and Ddc/R58E02-GAL4+ neurons, which mediate opposing behavioral responses to conditioned stimuli, generates an overlapping pattern of Ca^{2+} response plasticity in the γ lobe, with additional regions recruited by Ddc/R58E02-GAL4+ stimulation. Finally, (IV) the spatial pattern of plasticity coincides with differential sensitivity to cAMP in the γ lobe. Collectively, these data suggest that different subsets of neurons exhibit heterogeneous sensitivity to activation of second messenger signaling cascades, which may shape their responses to neuromodulatory network activity and modulate their propensity for recruitment into memory traces.

Our data suggest that dopaminergic neurons mediate Ca^{2+} response plasticity largely in the γ lobe, and suggest a potential mechanism for localization of short-term, learning-related plasticity. These data coincide with multiple previous studies that have demonstrated a critical role of γ neurons in short-term memory. Rescue of Rutabaga (Rut) in the γ lobe of *rut* mutants is sufficient to restore performance in short-term memory, while rescue in α/β lobes supports long-term memory [19, 36, 37]. Rescue of the D1-like DopR receptor in the γ lobe is sufficient to rescue both short- and long-term memory in a mutant background, suggesting that the γ neurons mediate the dopaminergic input during conditioning [34]. In addition, stimulating MP1 dopaminergic neurons innervating the heel of the γ lobe is

sufficient as an aversive reinforcer [17, 29]. Finally, learning induces plasticity in synaptic vesicle release from MB γ lobes, which depends in part on Gαo signaling [44]. Our data support a critical role for the γ lobe in short-term memory. Furthermore, the observation of differential sensitivity of the γ lobe to cAMP may provide an elegant explanation for why it is specifically recruited into short-term memory traces.

Direct elevation of cAMP was sufficient to generate localized, concentration-dependent Ca^{2+} response plasticity in the MB γ lobe in our experiments. Since applying forskolin in the bath is expected to elevate cAMP across the brain, the spatial specificity of the effect is remarkable. This was not an acute effect, as the forskolin was washed out before imaging the first post- conditioning odor response. At the concentrations we tested, only the γ lobe was facilitated. Therefore, we conclude that the γ lobe is most sensitive to elevation of cAMP, which has the effect of differentially recruiting γ neurons into the representation of short-term memory via dopamine-mediated neuronal plasticity. It is possible that additional signaling cascades are involved in generating learning-related plasticity in α/β and α′/β′ neurons [45], given that we did not observe Ca^{2+} response plasticity in those neurons following forskolin application.

The dominant model for cellular mechanisms of olfactory associative learning is that integration of information about the conditioned and unconditioned stimuli are integrated by Rut, which functions as a molecular coincidence detector [5, 26, 27]. This would suggest that MB neurons which receive CS and US information would exhibit at least somewhat uniform Ca^{2+} response plasticity. From this molecular/cellular perspective, the finding that the α/β and α′/β′ neurons did not exhibit Ca^{2+} response plasticity when an odor was paired with stimulation of dopaminergic neurons is surprising. These neurons are theoretically eligible to encode memory, as they receive information about the CS and US. However, as noted above, the finding that γ neurons differentially exhibit dopamine-dependent plasticity following single-cycle conditioning is consistent with the data from the behavioral experiments. In summary, the present results suggest that differential cAMP sensitivity provides a potential mechanism allowing specific subsets of eligible neurons in an array (γ neurons) to differentially encode CS-US coincidence relative to other subsets (α/β neurons) that also receive CS/US information.

EXPERIMENTAL PROCEDURES

Fly strains

Flies were cultured according to standard methods. Imaging was performed using the reporters GCaMP3, GCaMP6f, epac-camps, $^{T}epac^{VV}$, and AKAR3. The reporters were expressed in specific neuronal populations using either a MB enhancer or the GAL4-UAS system. Various GAL4 lines were used to drive expression of GAL4 in subsets of dopaminergic neurons, using a MB specific GAL80 repressor (MB-GAL80) to remove GAL4 expression in the MB when necessary.

Functional imaging

Isolated brain preparations were performed as previously described [26]. Dopamine was applied and washed out by switching the source of the bath perfusion solution for 30 s. *In vivo* functional imaging was performed as described previously [25]. The odorant ethyl butyrate was delivered through a stainless steel pipette mounted anterior to the fly's head. Temperature in the recording chamber was controlled with an inline Peltier element, monitored with a thermistor, and digitized. Forskolin, 1,9-dideoxyforskolin, and SCH-23390 (Tocris Bioscience) were applied in the bath.

Imaging and statistical analysis

Optical reporters were imaged with confocal microscopy using appropriate laser lines and emission filter settings on Leica TCS SP5 and SP8 confocal microscopes. Responses were plotted as the baseline-normalized change in GCaMP fluorescence ($\Delta F/F_0$), FRET ratio ($\Delta R/R_0$; AKAR3), or inverse FRET ratio ($\Delta R/R_0$; epac-camps, $^{T}epac^{VV}$). Statistical analysis was performed in Matlab (Mathworks) and Prism (Graphpad).

Supplementary Material

Refer to Web version on PubMed Central for supplementary material.

Acknowledgments

We thank Vivek Jayaraman, Kei Ito, Jay Hirsh, Brian Howell, Josh Dubnau, Scott Waddell, Hiromu Tanimoto, Gerald Rubin, Ronald L. Davis, Jacob Berry, Douglas Kim, and the Bloomington Drosophila Stock Center for fly stocks. We also thank Vivek Jayaraman and Loren Looger for providing the pMUH-GCaMP3 plasmid. Germain Busto and Isaac Cervantes-Sandoval provided helpful feedback on the manuscript. This research was supported by NIH/NIMH R00 MH092294.

References

1. Wise RA. Dopamine, learning and motivation. Nat Rev Neurosci. 2004; 5:483–494. [PubMed: 15152198]
2. Vergoz V, Roussel E, Sandoz JC, Giurfa M. Aversive learning in honeybees revealed by the olfactory conditioning of the sting extension reflex. PLoS One. 2007; 2:e288. [PubMed: 17372627]
3. Davis RL. Traces of Drosophila memory. Neuron. 2011; 70:8–19. [PubMed: 21482352]
4. Tomchik, SM.; Davis, RL. Memory Research Through Four Eras: Genetic, Molecular Biology, Neuroanatomy, and Systems Neuroscience. In: Menzel, R.; Benjamin, P., editors. Invertebrate Learning and Memory. London: Elsevier; 2013. p. 359-377.
5. Heisenberg M. Mushroom body memoir: from maps to models. Nat Rev Neurosci. 2003; 4:266–275. [PubMed: 12671643]
6. Hauber W. Involvement of basal ganglia transmitter systems in movement initiation. Prog Neurobiol. 1998; 56:507–540. [PubMed: 9775402]
7. Bromberg-Martin ES, Matsumoto M, Hikosaka O. Dopamine in motivational control: rewarding, aversive, and alerting. Neuron. 2010; 68:815–834. [PubMed: 21144997]
8. Andretic R, van Swinderen B, Greenspan RJ. Dopaminergic modulation of arousal in Drosophila. Curr Biol. 2005; 15:1165–1175. [PubMed: 16005288]
9. Lebestky T, Chang JS, Dankert H, Zelnik L, Kim YC, Han KA, Wolf FW, Perona P, Anderson DJ. Two different forms of arousal in Drosophila are oppositely regulated by the dopamine D1 receptor ortholog DopR via distinct neural circuits. Neuron. 2009; 64:522–536. [PubMed: 19945394]

10. Kenny PJ. Reward mechanisms in obesity: new insights and future directions. Neuron. 2011; 69:664–679. [PubMed: 21338878]
11. Zhang K, Guo JZ, Peng Y, Xi W, Guo A. Dopamine-mushroom body circuit regulates saliency-based decision-making in Drosophila. Science. 2007; 316:1901–1904. [PubMed: 17600217]
12. Doya K. Modulators of decision making. Nat Neurosci. 2008; 11:410–416. [PubMed: 18368048]
13. Schroll C, Riemensperger T, Bucher D, Ehmer J, Voller T, Erbguth K, Gerber B, Hendel T, Nagel G, Buchner E, et al. Light-induced activation of distinct modulatory neurons triggers appetitive or aversive learning in Drosophila larvae. Curr Biol. 2006; 16:1741–1747. [PubMed: 16950113]
14. Tanaka NK, Tanimoto H, Ito K. Neuronal assemblies of the Drosophila mushroom body. J Comp Neurol. 2008; 508:711–755. [PubMed: 18395827]
15. Mao Z, Davis RL. Eight different types of dopaminergic neurons innervate the Drosophila mushroom body neuropil: anatomical and physiological heterogeneity. Front Neural Circuits. 2009; 3:5. [PubMed: 19597562]
16. Claridge-Chang A, Roorda RD, Vrontou E, Sjulson L, Li H, Hirsh J, Miesenbock G. Writing memories with light-addressable reinforcement circuitry. Cell. 2009; 139:405–415. [PubMed: 19837039]
17. Aso Y, Siwanowicz I, Bracker L, Ito K, Kitamoto T, Tanimoto H. Specific dopaminergic neurons for the formation of labile aversive memory. Curr Biol. 2010; 20:1445–1451. [PubMed: 20637624]
18. Schwaerzel M, Monastirioti M, Scholz H, Friggi-Grelin F, Birman S, Heisenberg M. Dopamine and octopamine differentiate between aversive and appetitive olfactory memories in Drosophila. J Neurosci. 2003; 23:10495–10502. [PubMed: 14627633]
19. Zars T, Fischer M, Schulz R, Heisenberg M. Localization of a short-term memory in Drosophila. Science. 2000; 288:672–675. [PubMed: 10784450]
20. Placais PY, Trannoy S, Isabel G, Aso Y, Siwanowicz I, Belliart-Guerin G, Vernier P, Birman S, Tanimoto H, Preat T. Slow oscillations in two pairs of dopaminergic neurons gate long-term memory formation in Drosophila. Nat Neurosci. 2012; 15:592–599. [PubMed: 22366756]
21. Berry JA, Cervantes-Sandoval I, Nicholas EP, Davis RL. Dopamine is required for learning and forgetting in Drosophila. Neuron. 2012; 74:530–542. [PubMed: 22578504]
22. Krashes MJ, DasGupta S, Vreede A, White B, Armstrong JD, Waddell S. A neural circuit mechanism integrating motivational state with memory expression in Drosophila. Cell. 2009; 139:416–427. [PubMed: 19837040]
23. Kaun KR, Azanchi R, Maung Z, Hirsh J, Heberlein U. A Drosophila model for alcohol reward. Nat Neurosci. 2011; 14:612–619. [PubMed: 21499254]
24. Bang S, Hyun S, Hong ST, Kang J, Jeong K, Park JJ, Choe J, Chung J. Dopamine signalling in mushroom bodies regulates temperature-preference behaviour in Drosophila. PLoS Genet. 2011; 7:e1001346. [PubMed: 21455291]
25. Tomchik SM. Dopaminergic neurons encode a distributed, asymmetric representation of temperature in Drosophila. J Neurosci. 2013; 33:2166–2176a. [PubMed: 23365252]
26. Tomchik SM, Davis RL. Dynamics of learning-related cAMP signaling and stimulus integration in the Drosophila olfactory pathway. Neuron. 2009; 64:510–521. [PubMed: 19945393]
27. Gervasi N, Tchenio P, Preat T. PKA dynamics in a Drosophila learning center: coincidence detection by rutabaga adenylyl cyclase and spatial regulation by dunce phosphodiesterase. Neuron. 2010; 65:516–529. [PubMed: 20188656]
28. Kim YC, Lee HG, Han KA. D1 dopamine receptor dDA1 is required in the mushroom body neurons for aversive and appetitive learning in Drosophila. J Neurosci. 2007; 27:7640–7647. [PubMed: 17634358]
29. Aso Y, Herb A, Ogueta M, Siwanowicz I, Templier T, Friedrich AB, Ito K, Scholz H, Tanimoto H. Three dopamine pathways induce aversive odor memories with different stability. PLoS Genet. 2012; 8:e1002768. [PubMed: 22807684]
30. Liu C, Placais PY, Yamagata N, Pfeiffer BD, Aso Y, Friedrich AB, Siwanowicz I, Rubin GM, Preat T, Tanimoto H. A subset of dopamine neurons signals reward for odour memory in Drosophila. Nature. 2012; 488:512–516. [PubMed: 22810589]

31. Burke CJ, Huetteroth W, Owald D, Perisse E, Krashes MJ, Das G, Gohl D, Silies M, Certel S, Waddell S. Layered reward signalling through octopamine and dopamine in Drosophila. Nature. 2012; 492:433–437. [PubMed: 23103875]
32. Cervantes-Sandoval I, Martin-Pena A, Berry JA, Davis RL. System-like consolidation of olfactory memories in Drosophila. J Neurosci. 2013; 33:9846–9854. [PubMed: 23739981]
33. Krashes MJ, Keene AC, Leung B, Armstrong JD, Waddell S. Sequential use of mushroom body neuron subsets during drosophila odor memory processing. Neuron. 2007; 53:103–115. [PubMed: 17196534]
34. Qin H, Cressy M, Li W, Coravos JS, Izzi SA, Dubnau J. Gamma neurons mediate dopaminergic input during aversive olfactory memory formation in Drosophila. Curr Biol. 2012; 22:608–614. [PubMed: 22425153]
35. Yu D, Akalal DB, Davis RL. Drosophila alpha/beta mushroom body neurons form a branch-specific, long-term cellular memory trace after spaced olfactory conditioning. Neuron. 2006; 52:845–855. [PubMed: 17145505]
36. Blum AL, Li W, Cressy M, Dubnau J. Short- and long-term memory in Drosophila require cAMP signaling in distinct neuron types. Curr Biol. 2009; 19:1341–1350. [PubMed: 19646879]
37. Trannoy S, Redt-Clouet C, Dura JM, Preat T. Parallel processing of appetitive short- and long-term memories in Drosophila. Curr Biol. 2011; 21:1647–1653. [PubMed: 21962716]
38. Dubnau J, Chiang AS. Systems memory consolidation in Drosophila. Curr Opin Neurobiol. 2013; 23:84–91. [PubMed: 23084099]
39. Pech U, Pooryasin A, Birman S, Fiala A. Localization of the Contacts Between Kenyon Cells and Aminergic Neurons in the Drosophila melanogaster Brain Using SplitGFP Reconstitution. J Comp Neurol. 2013; 521:3992–4026. [PubMed: 23784863]
40. Friggi-Grelin F, Iche M, Birman S. Tissue-specific developmental requirements of Drosophila tyrosine hydroxylase isoforms. Genesis. 2003; 35:260–269. [PubMed: 12717737]
41. Dubnau J, Chiang AS, Grady L, Barditch J, Gossweiler S, McNeil J, Smith P, Buldoc F, Scott R, Certa U, et al. The staufen/pumilio pathway is involved in Drosophila long-term memory. Curr Biol. 2003; 13:286–296. [PubMed: 12593794]
42. Li H, Chaney S, Roberts IJ, Forte M, Hirsh J. Ectopic G-protein expression in dopamine and serotonin neurons blocks cocaine sensitization in Drosophila melanogaster. Curr Biol. 2000; 10:211–214. [PubMed: 10704417]
43. Sitaraman D, Zars M, Laferriere H, Chen YC, Sable-Smith A, Kitamoto T, Rottinghaus GE, Zars T. Serotonin is necessary for place memory in Drosophila. Proc Natl Acad Sci U S A. 2008; 105:5579–5584. [PubMed: 18385379]
44. Zhang S, Roman G. Presynaptic inhibition of gamma lobe neurons is required for olfactory learning in Drosophila. Curr Biol. 2013; 23:2519–2527. [PubMed: 24291093]
45. Wang Y, Mamiya A, Chiang AS, Zhong Y. Imaging of an early memory trace in the Drosophila mushroom body. J Neurosci. 2008; 28:4368–4376. [PubMed: 18434515]

HIGHLIGHTS

- Dopaminergic neurons drive compartmentalized elevation of postsynaptic cAMP
- Broad dopaminergic stimulation generates discrete patterns of olfactory plasticity
- cAMP elevation drives nonlinear spatial patterns of postsynaptic plasticity
- Patterns of plasticity correlate with spatiotemporal involvement in memory

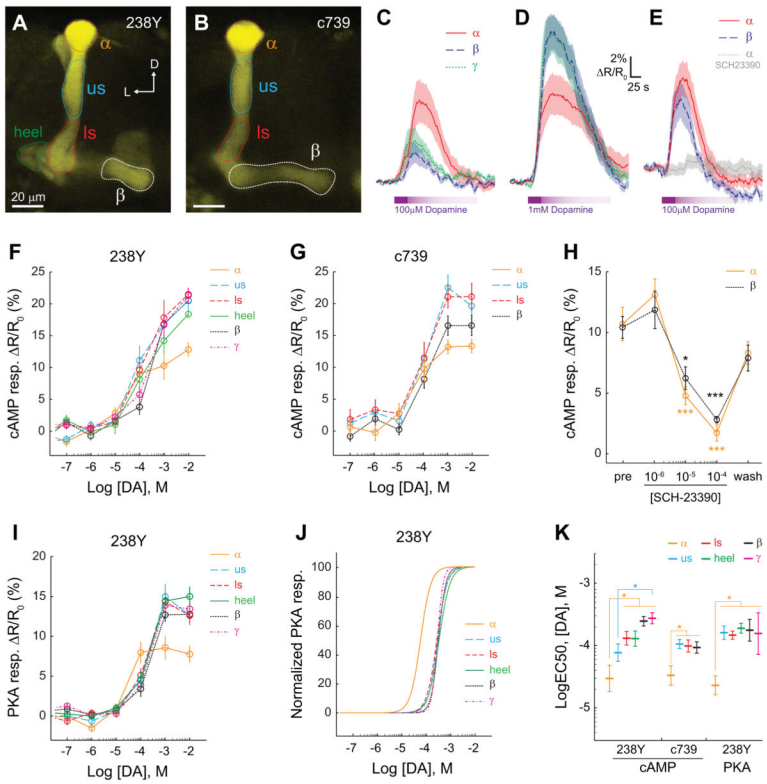

Figure 1. Dopamine elevates cAMP and PKA across multiple MB lobes

(A) Confocal image (single z plane) showing YFP fluorescence from the MB of a 238Y-GAL4>UAS-epac-camps fly. Regions of interest were placed at multiple levels of the α/β neurons (α tip, upper stalk, lower stalk), the heel, and the γ lobe (not visible at this plane of section). D: dorsal, L: lateral.

(B) A confocal image of the YFP fluorescence from the MB α/β neurons of a c739-GAL4>UAS-epac-camps fly, oriented as in panel A.

(C) Increases in cAMP observed in several regions of the MB following application of 100 μM dopamine in the bath in 238Y-GAL4>UAS-epac-camps flies (n ≥ 11). Lines and shaded regions represent the mean and S.E.M, respectively.

D) Increases in cAMP observed in several regions of the MB following application of 1 mM dopamine in the bath (n ≥ 11). Colors and lines are the same as in panel C.

(E) cAMP responses following application of 100 μM dopamine in the α and β lobes of c739-GAL4>UAS-epac-camps flies (n = 8) in the presence and absence of 100 μM SCH-23390.

(F) Dose-response curves showing the cAMP responses across multiple regions of interest in the MB to dopamine in 238Y-GAL4>UAS-epac-camps flies (n ≥ 8).

(G) Dose-response curves showing the cAMP responses across multiple regions of interest in the MB to dopamine in c739-GAL4>UAS-epac-camps flies (n ≥ 8).

(H) cAMP responses from the α and β lobes were inhibited by the addition of SCH-23390 in the bath in c739-GAL4>UAS-epac-camps flies (n = 8). The three concentrations were applied sequentially, and the responses recorded 10 min apart. There was a significant main

effect of treatment ($p < 0.001$; two-way repeated-measures ANOVA). *$p < 0.05$, **$p < 0.01$, ***$p<0.001$ (Sidak), relative to the pre-application response magnitudes.

(I) Dose-response curves showing the PKA responses across multiple regions of interest in the MB to dopamine in 238Y-GAL4>UAS-AKAR3 flies (n = 11 for concentrations ≥ 10^{-6} M, n = 6 for subthreshold concentrations).

(J) Normalized dose-response curves for the data in panel I.

(K) Quantification of the logEC50 of the AKAR3 responses to dopamine. *$p < 0.05$ (Tukey).

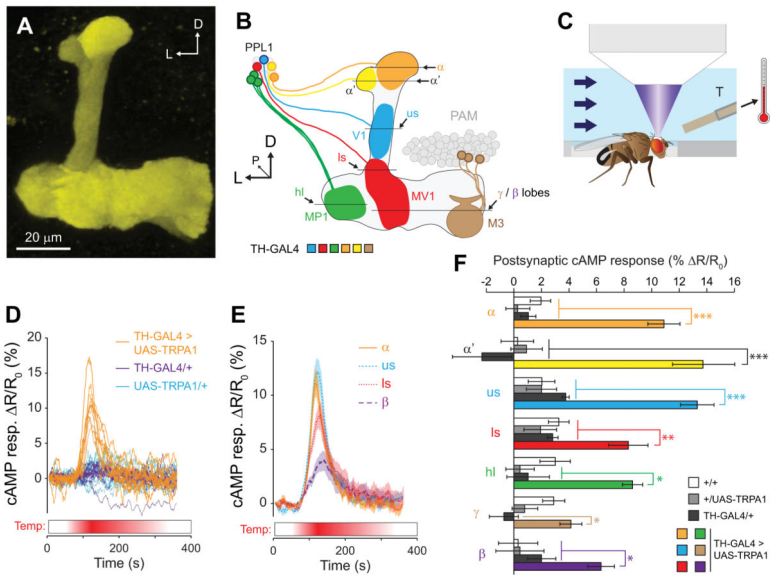

Figure 2. Stimulation of TH-GAL4+ dopaminergic neurons elevated cAMP across broad spatial regions of the MB

(A) Maximum intensity projection of a z stack of YFP fluorescence from a MB-^{T}epac^{VV} fly. D: doral, L: lateral.

(B) Schematic of the MB and PPL1 dopaminergic neurons, showing the z planes that were selected for imaging. Different dopaminergic neurons in the PPL1 cluster, all of which are labeled by the TH-GAL4 driver, are shown in different colors. D: dorsal, L: lateral, P: posterior, us: upper stalk, ls: lower stalk.

(C) Schematic of the *in vivo* imaging chamber, showing the fly's position relative to the thermistor, the microscope objective (not to scale), and the saline flow.

(D) Time series traces of ^{T}epac^{VV} responses to stimulation of dopaminergic neurons in TH-GAL4>UAS-TRPA1, MB- ^{T}epac^{VV} flies (heterozygous for all transgenes), as well as controls lacking the GAL4 or UAS elements. The lines represent the responses imaged in the upper stalk of individual flies (n = 12).

(E) Time series ^{T}epac^{VV} responses to thermogenetic stimulation (as in panel D), imaged from different regions of the MB. Lines and shaded regions represent the mean and S.E.M, respectively.

(F) Bar graphs of MB-^{T}epac^{VV} peak response magnitudes across different spatial regions of the MB (mean ± S.E.M.) following thermogenetic stimulation of TH-GAL4+ dopaminergic neurons (n ≥ 10). *p<0.05, **p<0.01, ***p<0.001 (Tukey).

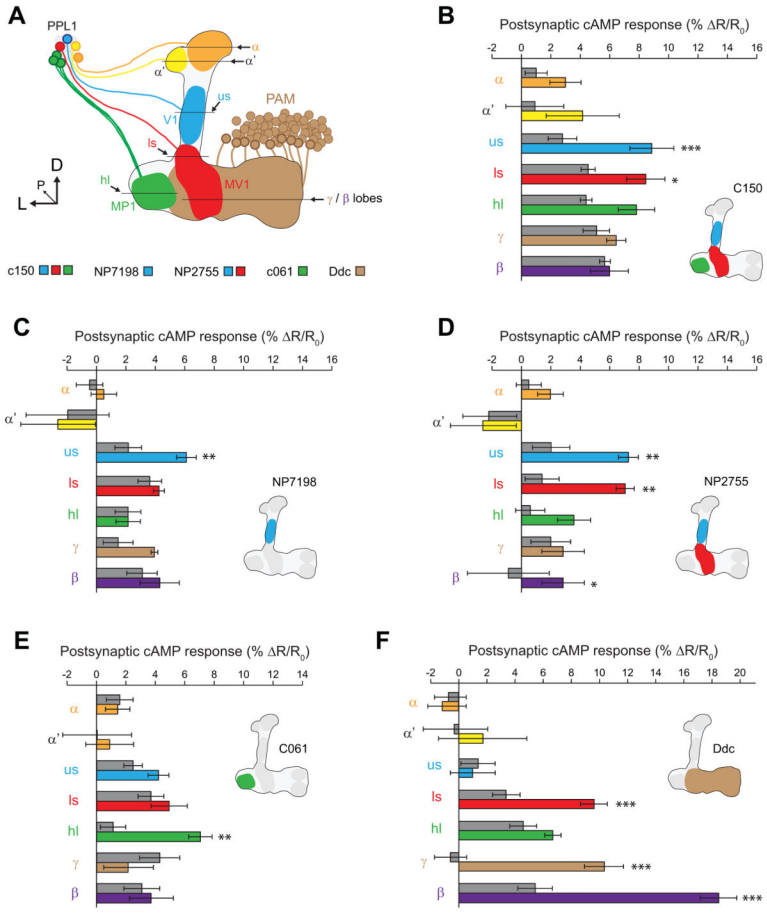

Figure 3. Stimulation of discrete subsets of dopaminergic neurons generated consistent compartmentalized elevation of cAMP across multiple spatial regions of the MB

(A) Schematic of the MB and extrinsic dopaminergic neurons, which are labeled by different GAL4 drivers. The β lobe (not shown) is posterior to the ventral γ lobe. D: dorsal, L: lateral, P: posterior, us: upper stalk, ls: lower stalk.

(B–F) Bar graphs of MB-^{T}epac^{VV} peak response magnitudes across different spatial regions of the MB (mean ± S.E.M.) following thermogenetic stimulation of different subsets of dopaminergic neurons (n ≥ 8). Colored bars indicate the responses from flies containing both the GAL4 and UAS-TRPA1 elements, with the specific colors referring to the region imaged as in panel (A). The adjacent gray bars are the GAL4/+ controls. *p<0.05, **p<0.01, ***p<0.001 (Tukey).

(B) C150-GAL4

(C) NP7198-GAL4

(D) NP2755-GAL4

(E) C061-GAL4

(F) Ddc-GAL4

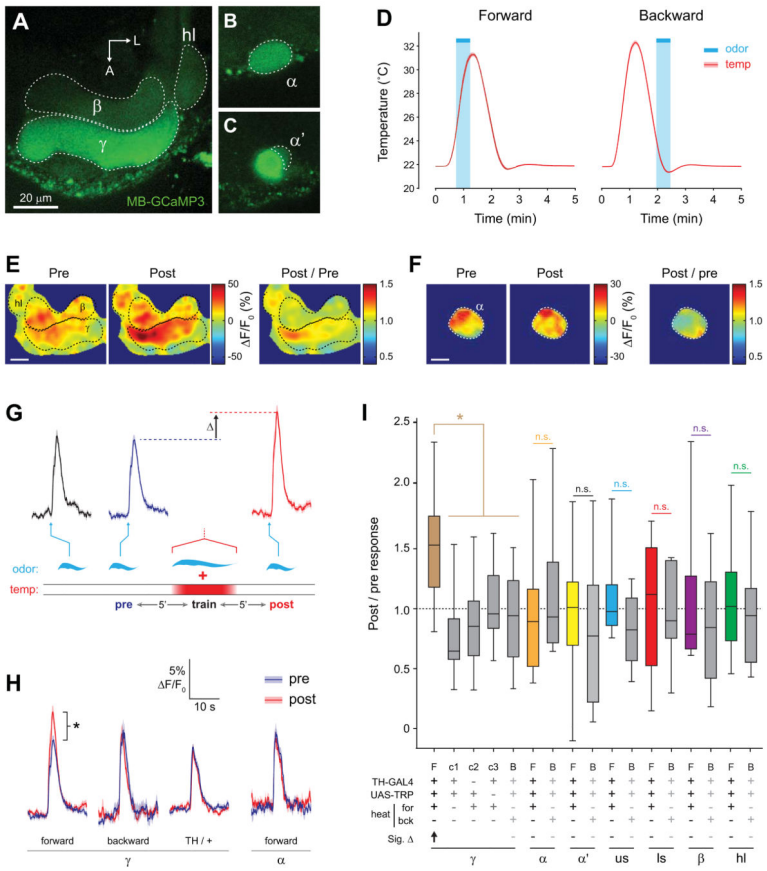

Figure 4. Conditioning with odor and TH-GAL4+ dopaminergic neuron stimulation yielded discrete facilitation in the MB γ lobe

(A) Confocal images of GCaMP fluorescence from a TH-GAL4>UAS-TRPA1, MB-GCaMP3 fly (heterozygous for all transgenes) *in vivo*. The plane of section shows the β and γ lobes of the MB, with corresponding regions of interest outlined.

(B) Confocal image as in panel (A), with a z plane showing the α tip (dashed outline).

(C) Confocal image as in panel (A), with a z plane showing the α' tip (dashed outline).

(D) Temperature (mean ± S.E.M.) measured in the bath adjacent to the fly's head during forward and backward conditioning. The 30-s odor delivery time is superimposed.

(E) Pseudocolor images of the odor responses in the β and γ lobes before and after conditioning from a representative fly using the TH-GAL4 driver. Scale bar = 10 µm.

(F) Pseudocolor images of the odor responses in the α tip before and after conditioning from a representative fly. Scale bar = 10 µm.

(G) GCaMP responses (mean ± S.E.M.) to odor for the time points measured. The odor presentations immediately before and after conditioning are marked "pre" and "post". The scale matches panel (H). Odor presentations were spaced 5 min apart (5′).

(H) Comparison of pre- and post- conditioning odor responses for several genotypes, conditioning paradigms, and MB regions (n ≥ 10). *p < 0.05 (Mann-Whitney).

(I) The post / pre odor response ratio for all genotypes, conditioning paradigms, and MB regions (n ≥ 10). There was a significant effect across groups (p < 0.001; Kruskal-Wallis). *p<0.05 (Mann-Whitney); n.s.: not significant. In the legend below the figure, Sig. Δ

indicates significant change in odor-evoked ΔF/F following conditioning within each group, with direction indicated by arrow (Wilcoxon signed-rank tests; $p < 0.05$). F: forward, B: backward, c1: control 1 (no heat), c2: control 2 (no GAL4), c3: control 3 (no TRPA1), us: upper stalk, ls: lower stalk, hl: heel.

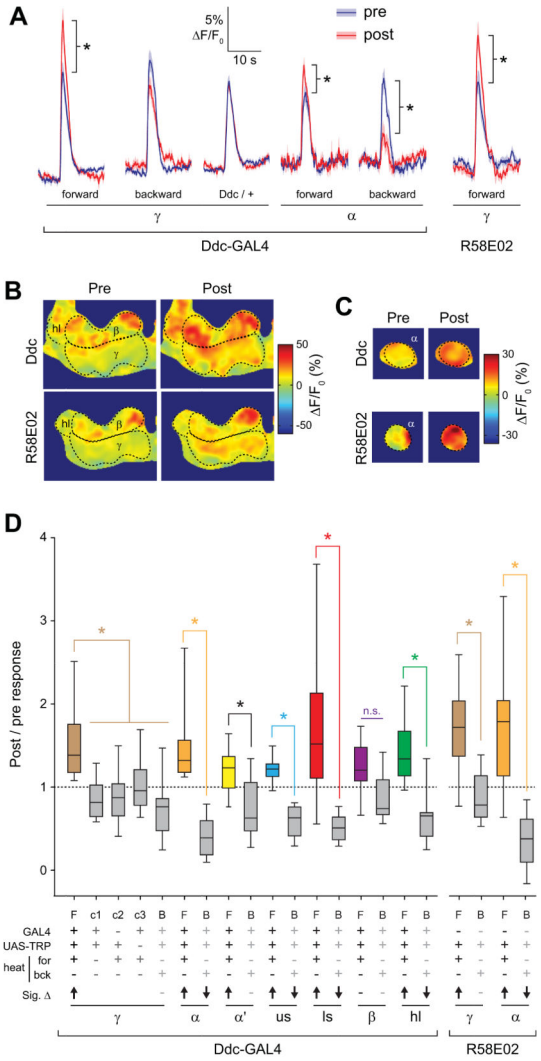

Figure 5. Conditioning with PAM dopaminergic neurons stimulation yielded broad, bidirectional Ca^{2+} response plasticity across the MB

(A) Comparison of pre- and post- conditioning odor responses for several genotypes, conditioning paradigms, PAM-specific GAL4 lines (Ddc and R58E02), and MB regions ($n \geq 10$). *$p < 0.05$ (Mann-Whitney).

(B) Pseudocolor images of the odor responses in the β and γ lobes before and after conditioning from a representative fly using the Ddc- and R58E02-GAL4 drivers. Scale bar = 10 μm.

(C) Pseudocolor images of the odor responses in the α tip before and after conditioning from a representative fly. Scale bar = 10 μm.

(D) The post / pre odor response ratio for all genotypes, conditioning paradigms, and MB regions ($n \geq 10$). There was a significant effect across groups ($p < 0.001$; Kruskal-Wallis). *$p<0.05$ (Mann-Whitney); n.s.: not significant. In the legend below the figure, Sig. Δ indicates significant change in odor-evoked ΔF/F following conditioning within each group, with direction indicated by arrow (Wilcoxon signed-rank; $p < 0.05$). F: forward, B:

backward, c1: control 1 (no heat), c2: control 2 (no GAL4), c3: control 3 (no TRPA1), us: upper stalk, ls: lower stalk, hl: heel.

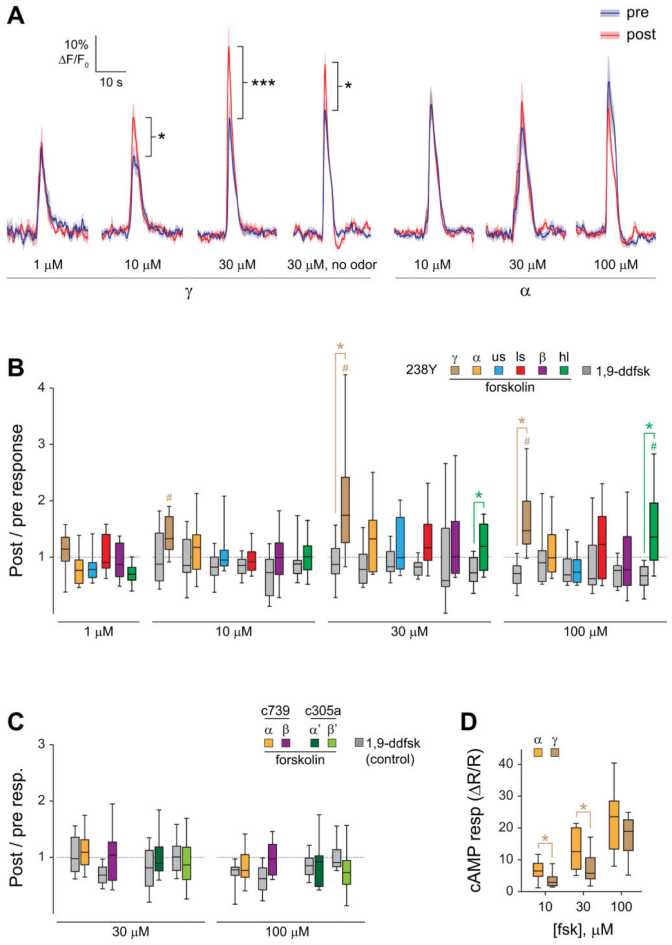

Figure 6. Elevating cAMP broadly with forskolin revealed localized Ca^{2+} response plasticity in the γ lobe

(A) Comparison of odor responses before and after pairing of odor with forskolin application, or presenting forskolin alone, in 238Y-GAL4>UAS-GCaMP6f flies ($n \geq 12$). *$p < 0.05$, ***$p < 0.001$ (Wilcoxon signed-rank test for no odor group, Sidak following ANOVA for all others).

(B) Box plots graphing the change in magnitude of odor responses across different MB regions following pairing of odorant with forskolin (colors) or 1,9-didexyforskolin (gray) in 238Y-GAL4>UAS-GCaMP6f flies ($n \geq 12$). Odor responses were significantly elevated following forskolin treatment in the γ lobe at 10, 30, and 100 μM and the heel at 100 μM (# $p < 0.05$; Wilcoxon signed-rank tests). Forskolin-treated animals showed a significantly larger post / pre odor responses than 1,9-dideoxyfoskolin-treated animals in the γ lobe and heel at 30 μM and 100 μm (*$p < 0.05$; Mann-Whitney).

(C) Imaging the effects of elevating cAMP in the α, α′, β, and β′ regions with specific drivers (c739-GAL4 for MB α/β neurons and c305a-GAL4 for MB α′/β′ neurons). Box plots are graphed as in panel B. There were no significant differences in post/pre odor response ratios between forskolin and 1,9-dideoxyforskolin groups in any region (Mann-Whitney).

(D) Forskolin (fsk) increased cAMP in both the α tip and γ lobe. The response magnitudes were significantly different (with the α lobe showing larger median increases) between these regions at 10 μM and 30 μM ($p < 0.001$; Friedman; $^*p < 0.05$; $n = 13$; Wilcoxon signed-rank), but not 100 μM.